



Full Length Article

Antimicrobial photodynamic therapy improves the alveolar repair process and prevents the occurrence of osteonecrosis of the jaws after tooth extraction in senile rats treated with zoledronate



Edilson Ervolino^{a,b,f,*}, Cristian Statkiewicz^c, Luan Felipe Toro^{b,f}, João Martins de Mello-Neto^{c,f}, Thamires Priscila Cavazana^d, João Paulo Mardegan Issa^e, Rita Cássia Menegati Dornelles^a, Juliano Milanezi de Almeida^c, Maria José Hitomi Nagata^c, Roberta Okamoto^{a,c}, Cláudio Aparecido Casatti^a, Valdir Gouveia Garcia^{c,f}, Leticia Helena Theodoro^{c,f}

^a São Paulo State University (UNESP), School of Dentistry, Department of Basic Sciences, Rua José Bonifácio, 1193, CEP 16015-050, Araçatuba, SP, Brazil

^b São Paulo State University (UNESP), Institute of Biosciences, Rua Prof. Dr. Antônio Celso Wagner Zanin, 250, CEP 18618-689, Botucatu, SP, Brazil

^c São Paulo State University (UNESP), School of Dentistry, Department of Surgery and Integrated Clinic, Rua José Bonifácio, 1193, CEP 16015-050, Araçatuba, SP, Brazil

^d São Paulo State University (UNESP), School of Dentistry, Department of Pediatric Dentistry and Public Health, Rua José Bonifácio, 1193, CEP 16015-050, Araçatuba, SP, Brazil

^e São Paulo University (USP), School of Dentistry, Department of Morphology, Physiology and Basic Pathology, Avenida do Café, s/n, CEP 14040-904, Ribeirão Preto, SP, Brazil

^f Group for the Research and Study of Laser in Dentistry, São Paulo State University (UNESP), School of Dentistry, Rua José Bonifácio, 1193, CEP 16015-050, Araçatuba, SP, Brazil

ARTICLE INFO

Keywords:

Bisphosphonate-related osteonecrosis of the jaws

Photochemotherapy

Prevention

Tooth socket

Wound healing

ABSTRACT

This study evaluated the effects of antimicrobial photodynamic therapy (aPDT) in the alveolar repair of rats with major risk factors for bisphosphonate-related osteonecrosis of the jaws (BRONJ). Senile rats received 0.45 ml of vehicle (VEH and VEH/aPDT) or 0.45 ml of zoledronate (ZOL and ZOL/aPDT) every three days for seven weeks. After three weeks of treatment, the first lower left molar was extracted. VEH/aPDT and ZOL/aPDT were submitted to aPDT on the extraction site at 0, 2 and 4 days postoperatively. Euthanasia was performed 28 days postoperatively and the extraction site was evaluated by clinical, histological, histometric, histochemical and immunohistochemical analysis. ZOL showed tissue repair impairment; lower percentage of newly formed bone tissue (NFBT); higher percentage of non-vital bone tissue (NVBT); fewer mature collagen fibers and increased immunolabeling for tumor necrosis factor (TNF α), interleukin (IL)-1 β and IL-6. ZOL/aPDT showed clinical and histological characteristics of the extraction site, percentage of NFBT and percentage of mature collagen fiber similar to VEH. Percentage of NVBT and immunolabeling for inflammatory cytokines in ZOL/aPDT was lower than in ZOL. Immunolabeling for tartarato-resistant acid phosphatase (TRAP) was lower in ZOL and ZOL/aPDT. aPDT in the dental extraction site improves tissue repair process and prevents the occurrence of BRONJ-like lesions after tooth extraction.

1. Introduction

Bisphosphonates (BPs) are antiresorptive drugs used for treatment of diseases that trigger osteopenia/osteoporosis or lytic bone lesions [1,2]. A severe adverse effect caused by such drugs is bisphosphonate-related osteonecrosis of the jaws (BRONJ) [3]. The American Association of Oral and Maxillofacial Surgery (AAOMS) defines this condition as presence of exposed bone in the maxillofacial region for a period longer than eight weeks in patients submitted to previous or current

treatment with BPs and no history of radiotherapy in the jaws [4]. The incidence of BRONJ is approximately 0.01% in patients making use of oral BPs, and about 12% in patients taking BPs intravenously [5–7]. Epidemiological studies have shown that BRONJ has been prevalently observed in older women. Zoledronate is associated with most cases of this pathology. BRONJ tends to occur in the jaw, specifically in pre-molar and molar regions, having tooth extraction as one of the main triggers [5–7].

The pathogenesis of BRONJ is still poorly understood, making its

* Corresponding author at: Rua José Bonifácio, 1193, CEP 16015-050, Araçatuba, SP, Brazil.

E-mail address: e.ervolino@unesp.br (E. Ervolino).

<https://doi.org/10.1016/j.bone.2018.10.014>

Received 25 June 2018; Received in revised form 26 September 2018; Accepted 15 October 2018

Available online 16 October 2018

8756-3282/ © 2018 Elsevier Inc. All rights reserved.

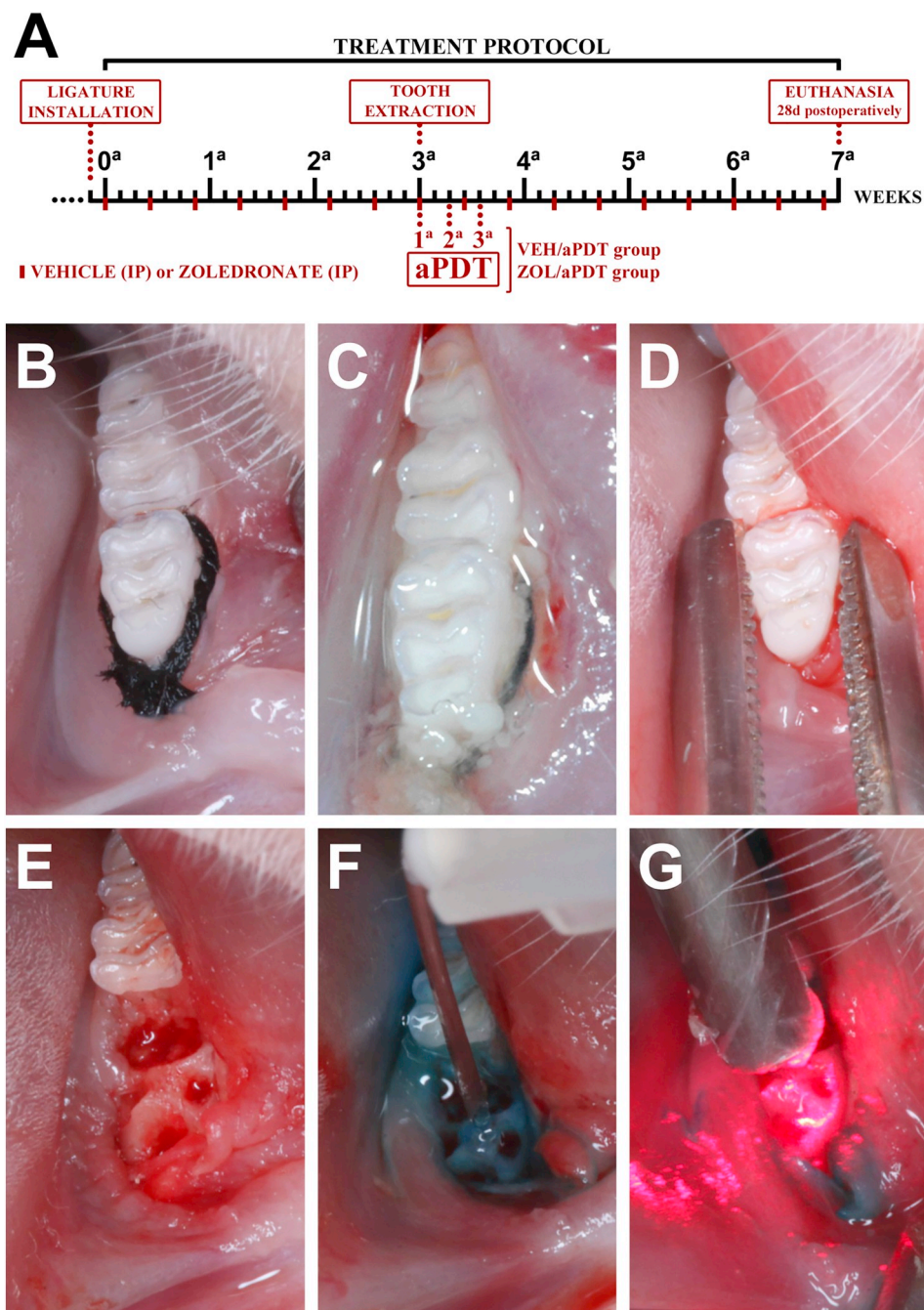


Fig. 1. Experimental design. A: scheme illustrating experimental procedures performed during the study. B: ligature installed in lower first molar to induce experimental periodontitis. C: experimental periodontitis induced three weeks after ligation installation. D: surgical procedure for tooth extraction. E: clinical aspect of extraction site. F–G: aPDT in extraction site (in F, photosensitizing agent deposition, in G, laser irradiation).

prevention and treatment difficult. Several etiopathological factors have been identified as possible triggers of BRONJ, including: i) potent suppression of resorptive osteoclasts activity, resulting in accumulation of bone microfractures, increasing the presence of non-vital bone tissue areas; ii) potent anti-angiogenic effects of BPs, resulting in avascular bone necrosis; iii) BPs cytotoxic effects, decreasing the repair ability of both soft and hard tissues; iv) increased susceptibility to infection of bone tissue; v) dysfunction of the local immune response [4,8–11].

BRONJ treatment has been carried out by different clinical approaches, solely based on clinical staging of the disease, following different protocols such as mouthwash with 0.12% chlorhexidine gluconate, and/or prolonged antibiotic therapy and/or surgical debridement of lesion, which in severe cases may consist of partial or complete

mandibulectomy/maxillectomy [12–14]. Currently, prescription of antibiotic prophylaxis has also been recommended for patients under long-term treatment with BPs, who require invasive dental interventions, especially tooth extractions [15]; however, this preventive therapy may sometimes fail. Effective and safe therapies for BRONJ treatment are still needed. In this context, experimental models of BRONJ-like lesions may contribute to the proposal and evaluation of preventive and/or curative therapies, and therefore guide clinical research.

Antimicrobial photodynamic therapy (aPDT) exerts positive effects at the cellular and tissue level, which places it as a potential preventive therapy for BRONJ. The aPDT consists in employing an appropriate wavelength of light to excite a photosensitizer (PS), which is pre-

absorbed selectively by microbial cells. Under appropriate irradiation the PS changes from a lower energy level (ground singlet state, ^1PS) to a short-lived excited singlet state ($^1\text{PS}^*$), which can be converted to long-lived excited triplet state ($^3\text{PS}^*$) [16,17]. In the presence of oxygen, $^3\text{PS}^*$ can generate high levels of reactive oxygen species (ROS) by two mechanisms: via electron transfer to form predominantly superoxide radicals, hydroxyl radicals, hydrogen peroxide (mechanism type I) or via energy transfer to ground state triplet oxygen to produce highly reactive singlet oxygen ($^1\text{O}_2$) (mechanism type II) [16,17]. These high levels of generated ROS are highly cytotoxic, killing microbial cells that absorbed the PS [16,17]. Besides its antimicrobial action, studies have shown that when low-level laser is employed in aPDT as source of light, it presents photobiomodulatory effects, such as modulation of inflammatory response, angiogenesis, proliferation, migration, differentiation and cellular activity, which are essential events for the tissue repair process [18–20].

It was reported that aPDT has proven an effective treatment to control the microbial environment in the tooth socket after molar extraction with experimental periodontitis, which would favor the tissue repair process [21]. Clinical studies in humans showed that aPDT acts by accelerating the tissue repair process after tooth extraction while minimizing the undesirable symptoms and postoperative complications [22–24]. In view of these considerations, the present study evaluated the effects of multiple aPDT sessions in the tooth extraction site in rats with major risk factors for BRONJ. It was hypothesized that aPDT used on the extraction sites in senile female rats treated with zoledronate would improve alveolar repair and prevent the occurrence of BRONJ-like lesions after tooth extraction.

2. Material and methods

2.1. Animals and treatment protocols

Twenty-eight senile (20-month-old) female rats (*Rattus norvegicus* - Wistar) were used in this study. The experimental protocol was performed in compliance with the relevant laws and institutional guidelines in accordance with the ethical standards of the Declaration of Helsinki and approved by the Institutional Ethics Committee on Animal Use (#00581-2013 FOA – UNESP, Araçatuba/SP, Brazil).

All experimental procedures involving pain or discomfort to the animals were performed under anesthesia with ketamine hydrochloride (80 mg/kg, Francotar®, Virbac, SP, Brazil) and xylazine (10 mg/kg, Rompum®, Bayer, RS, Brazil).

One day prior to the beginning of the drug treatment plan, a cotton ligature (cotton thread # 24, Linhas Corrente®, SP, Brazil) was placed around the lower left first molar (Fig. 1A, B) in all animals. The purpose of the ligature installation was to induce experimental periodontitis (Fig. 1C) [20].

Subsequently, the rats were randomly distributed into four experimental groups and submitted to a seven-week drug treatment plan. VEH ($n = 7$) and VEH/aPDT ($n = 7$) groups were treated with vehicle. ZOL ($n = 7$) and ZOL/aPDT ($n = 7$) groups were treated with zoledronate (Chemical® Sigma, St. Louis, MO, USA). The treatment with vehicle or zoledronate was performed by the intraperitoneal route every three days (Fig. 1A). The vehicle consisted of 0.45 ml of 0.9% sodium chloride solution. The zoledronate dose was 100 mg/kg, diluted in vehicle. This dose and the drug treatment plan were based on protocol currently used to complement oncological therapy in humans, adapted to rats [20,25].

After three weeks of drug treatment, the cotton ligature was removed and the lower left first molar tooth was extracted. For exodontia, the animals were positioned on an operating table and antisepsis of the buccal cavity was performed with 10% povidone-iodine. Subsequently, syndesmotomy (circumferential sectioning of the supracrestal fibers of the gingiva), luxation (Fig. 1D) and extraction (Fig. 1E) of the lower left first molar were performed using adapted surgical tools [20].

In VEH and ZOL groups no local treatment was performed in the tooth extraction site. In VEH/aPDT and ZOL/aPDT groups three sessions of aPDT were performed at the tooth extraction site at 0, 2 and 4 postoperative days (Fig. 1A).

For aPDT, methylene blue (100 µg/ml) was employed as PS [26]. Five hundred microliters of PS was deposited and kept on the tooth extraction site for 60 s (Fig. 1F). Subsequently, the laser tip was positioned at a single point in the center of the tooth extraction site, parallel with the long axis of the tooth socket and in contact with the treated area (Fig. 1G). For low-level laser irradiation, an InGaAlP laser device (660 nm; Thera Lase®, DMC Equipamentos Ltda®, SP, Brazil) with spot size of 0.0283 cm² was used, following the parameters: 35 mW power; continuous operation mode; energy point of 2.1 J/point for 60 s, density energy of 74.2 J/cm²; power intensity of 1.23 W/cm² [20].

2.2. Collection and histological processing of samples

Euthanasia was performed 28 days after tooth extraction by transcardiac perfusion with 100 ml physiological saline solution added with 0.1% heparin and 800 ml of 4% formaldehyde (Chemical® Sigma, St. Louis, MO, USA) in phosphate buffered saline (PBS - Chemical® Sigma), 0.1 M, 4 °C, pH 7.4. The hemimandibles were dissected, post-fixed for 72 h and decalcified in 10% ethylenediamine tetra acetic acid (EDTA) (Chemical® Sigma) in PBS 0.1 M, pH 7.4 for 60 days.

Samples were dehydrated in a graded ethanol series (70°–80°–90°–95°–100°–100°–100° GL), cleared in xylene, infiltrated and embedded in paraffin. The histologic sections (4 µm thickness) were obtained in the sagittal plane, from the vestibular to the lingual surfaces of the mandible. Serial histological sections of the tooth extraction site formerly occupied by the roots of the mesial and distal left first molars were collected in proper glass slides.

The first histological section series was stained with hematoxylin-eosin (HE) for histological analysis of the tooth extraction site and adjacent tissues, and for histometric analysis of newly formed bone tissue (NFBT) and non-vital bone tissue (NVTB). The second histological section series was submitted to 0.1% picosirius red staining for analysis of the maturation level of collagen fibers under polarized microscopy [27].

Additional histological section series were submitted to indirect immunoperoxidase for detection of tartarato-resistant acid phosphatase (TRAP), tumor necrosis factor (TNF) α, interleukin (IL)-1β and IL-6. The histological sections were cleared in xylene and hydrated in a graded ethanol series (100°–100°–100°–95°–70° GL). The histological sections were submitted to heat-induced epitope retrieval (HIER) method using citrate buffer (Diva decloaker, Biocare Medical, Concord, CA, EUA) and pressure chamber (Decloaking chamber, Biocare Medical, Concord, CA, EUA) at 95 °C for 20 min. Next, the histological sections were washed in PBS 0.1 M, pH 7.4 and blocking of endogenous peroxidase and non-specific binding sites were done using 3% hydrogen peroxide for 1 h and 1% bovine serum albumin for 12 h, respectively. Histological sections from each experimental group were divided into four sets, and each set was incubated with one of the following primary antibodies: goat anti-TRAP (SC-30833, Santa Cruz Biotechnology®, TX, USA), goat anti-TNFα (SC-1348, Santa Cruz Biotechnology®), goat anti-IL-1β (SC-1252, Santa Cruz Biotechnology®) and rabbit anti-IL-6 (SC-1265, Santa Cruz Biotechnology®). Then, the histological sections were incubated with biotinylated secondary antibody for 90 min and subsequently with streptavidin conjugated with horseradish peroxidase (HRP) for 90 min (Universal Dako Labeled HRP Streptavidin-Biotin Kit, Dako Laboratories, CA, EUA). The immunoperoxidase was developed using 3,3'-diaminobenzidine tetrahydrochloride (DAB chromogen Kit, Dako Laboratories, CA, EUA). TRAP immunolabeled slides were counterstained with Harris' hematoxylin; while the remaining (TNFα, IL-1β e IL-6) slides were not submitted to counterstaining in order to avoid interference during immunolabeling optical density analysis. Finally, the histological sections were then dehydrated in ethanol, cleared in

xylene and covered in mounting medium (Permount, Fisher Scientific, San Diego, CA, USA) and glass coverslips. As negative control, the specimens were submitted to the same procedures, eliminating the use of the primary antibody.

2.3. Analysis of the results

2.3.1. Analysis of the general health condition and intraoral clinical examination

The general health condition of the animals was observed throughout the experimental period and body weight was weekly monitored. Intraoral clinical examination was performed, consisting of a detailed visual inspection of the oral cavity, in particular, of the tooth extraction site. The clinical parameters evaluated followed those established by Statkiewicz et al. [20].

2.3.2. Microscopic analysis and region of interest (ROI)

Microscopic analyzes were performed by a certified histologist blinded to treatments. For histological and histometric analyzes, three histological sections located on the buccal, middle and lingual portion of the tooth extraction site were evaluated. A histological section of the middle portion of the tooth extraction site was used for histochemical and immunohistochemical analysis.

In the present study, ROI (I) and ROI (II) were considered according to the performed microscopic analysis. ROI (I) consisted of a 4 mm × 4 mm area which included the portion of the tooth extraction site formerly occupied by the mesial and distal roots of the lower left first molar and adjacent tissues. Its distal limit consisted of a line situated parallel to the coronary dentin and root surface of the lower left second molar, extending 4 mm mesially. Its coronary limit consisted of a line parallel to the gingival margin-cement boundary of the lower left second molar, extending 4 mm apically [20]. ROI (II) consisted of two 250 × 250 μm areas, situated in the connective tissue overlying the tooth extraction site. The situation of these areas followed a line located at the center of the connective tissue, perpendicular to the long axis of the teeth and that divided such tissue in its coronal apical direction. Two other lines were used, one parallel to the central portion of the tooth extraction site formerly occupied by the mesial root and another one parallel to the central portion of the tooth extraction site formerly occupied by the distal root of the first molar. The intersection of these lines determined the center of the two analyzed areas [20].

2.3.3. Histological analysis of the tooth extraction site and adjacent tissues

Histological analysis was based on Statkiewicz et al. [20]. The following parameters were evaluated by optical microscopy in ROI (I): 1) intensity of local inflammatory response; 2) extension of inflammatory process; 3) cellular and structure pattern of epithelial tissue; 4) cellular and structure pattern of connective tissue; 5) cellular and structure pattern of bone and tissue; 6) contamination pattern of tooth extraction site.

2.3.4. Histometrical analysis of NFBT and NVBT

In ROI (I), images were captured by using a digital camera (AxioCam® Carl Zeiss, Gottingen, Germany) coupled to a light microscope (AxioLab®) and connected to a microcomputer. The total amount of bone tissue was calculated using image analysis software (Axiovision 4.8.2® Carl Zeiss). Next, the percentage of newly formed bone (NFBT) and percentage of non-vital bone tissue (NVBT) were calculated using the same software. The NVBT consisted of a region where more than ten lacunae of neighboring osteocytes were empty or containing remnants of necrotic osteocytes [28].

2.3.5. Histochemical analysis of the level of maturation of collagen fibers

In ROI (II), images were captured by using a digital camera (AxioCam® Carl Zeiss, Gottingen, Germany) coupled to a microscope equipped with a cross-polarizer (AxioLab®) and connected to a

microcomputer. The histochemical analysis of the maturation level of collagen fibers was evaluated by image analysis software (Axiovision 4.8.2® Carl Zeiss). The area occupied by the different colors, considering yellow-greenish staining as immature collagen fibers, and orange-red staining as mature collagen fibers was measured [27,29]. These values were expressed in percentages as mean ± standard deviation.

2.3.6. Immunohistochemical analysis

In ROI (I), images of histological sections immunolabeled with TRAP were collected as previously described. TRAP-positive cells per mm² and TRAP-positive cells per mm in the vital bone tissue were quantified using image analysis software (Axiovision 4.8.2® Carl Zeiss). The amount of TRAP-positive cells was expressed as mean ± standard deviation.

In ROI (II), images of histological sections immunolabeled with TNFα, IL-1β and IL-6 were obtained, as described above. The area corresponding to immunolabeling was obtained through optical density immunolabeling using a color threshold tool of image analysis software (Axiovision 4.8.2® Carl Zeiss) [30]. The data were expressed in percentages as mean ± standard deviation.

2.3.7. Statistical analysis

Statistical analyses were made using Bioestat 5.3 software program (Mamirua Institute, Manaus, AM, Brazil). The sample size was calculated to ensure the 95% statistical test power ($p < 0.05$). Shapiro-Wilk test was used for analysis of the normal distribution of data. Clinical and histological data were evaluated by nonparametric Kruskal-Wallis analysis of variance test and Student-Newman-Keuls post-test. Histometrical (NFBT and NVBT), histochemical (mature collagen fibers) and immunohistochemical (TRAP per mm², TRAP per mm, TNFα, IL-1β and IL-6) data were evaluated by analysis of variance (ANOVA) and Tukey's post-test. P value < 0.05 was considered statistically significant.

3. Results

3.1. General health condition and intraoral clinical examination

The general health conditions of the animals remained constant throughout the experimental period. These animals tolerated the surgical procedure of first molar extraction performed in all experimental groups, as well as the three aPDT sessions carried out in groups VEH/aPDT and ZOL/aPDT. At the end of the experimental period, there was no statistically significant difference in mean body weight among VEH (350 ± 5 g), VEH/aPDT (346 ± 7 g), ZOL (342 ± 7 g) and ZOL/aPDT (350 ± 7 g) groups. There was no statistically significant difference in intragroup body weight throughout the experimental period.

The oral clinical exam showed no macroscopic changes in the oral cavity or in the tooth extraction site at VEH, VEH/aPDT and ZOL/aPDT. However, the size of the surgical sites appeared larger in ZOL when compared to other experimental groups. In addition, some animals from ZOL group showed oral bone exposure in the tooth extraction site and adjacent tissues (Table 1).

3.2. Repair tissue in the tooth extraction site and adjacent tissues

VEH, VEH/aPDT and ZOL/aPDT groups showed similar tissue repair process in the tooth extraction site and overlying mucosa (Fig. 2). In contrast, group ZOL had the tissue repair process severely compromised, consistent with a BRONJ-like lesion (Fig. 2). The parameters, scores and distribution of specimens according to histological analysis of tissue are presented in Table 2.

Table 1

Scores and distribution of specimens according to clinical analysis of tooth extraction site and adjacent sites in VEH, VEH/aPDT, ZOL and ZOL/aPDT groups at 28 postoperative days.

Clinical analysis	Number of specimens			
	Experimental groups			
	VEH (n = 7)	VEH/aPDT (n = 7)	ZOL (n = 7)	ZOL/aPDT (n = 7)
Clinical aspect of tooth extraction site and adjacent tissues				
(1) Absence of exposed bone and totally repaired mucous membrane	7	7	–	6
(2) Absence of exposed bone and partially repaired mucous membrane	–	–	–	1
(3) BRONJ-like lesions – large extraction site with small area of exposed bone (less than half of the alveolar space) and impairment of mucous membrane repair	–	–	3	–
(4) BRONJ-like lesions – large extraction site with great area of exposed bone (more than half of the alveolar space) and impairment of mucous membrane repair	–	–	4	–
Median	1	1	4 ^{†‡}	1 [¶]

Symbols: †, statistically significant difference in relation to VEH; ‡, statistically significant difference in relation to VEH/aPDT; ¶, statistically significant difference in relation to ZOL.

3.3. NFBT and NVBT in tooth extraction site and adjacent tissues

In the ZOL group, NFBT in the tooth extraction site was significantly lower than in the other groups. There was no statistically significant difference between VEH and ZOL/aPDT groups. In VEH/aPDT group, NFBT was significantly larger than in ZOL/aPDT and did not differ statistically from VEH (Fig. 3).

NVBT in ZOL and ZOL/aPDT groups was significantly higher than in VEH and VEH/aPDT. NVBT was significantly lower in ZOL/aPDT group than in ZOL. No statistically significant difference was found between VEH and VEH/aPDT groups (Fig. 4).

3.4. Maturation level of collagen fibers in mucosa overlying tooth extraction site

No statistically significant difference was observed between VEH and VEH/aPDT groups. The percentage of mature collagen fibers was lower in ZOL compared with the remaining groups. VEH/aPDT presented higher percentage of mature collagen fibers in comparison to ZOL/aPDT group. No statistically significant difference was observed between VEH and ZOL/aPDT groups (Fig. 5).

3.5. Immunolabeling pattern for TRAP, TNF α , IL-1 β and IL-6

The immunohistochemical technique used for detection of TRAP, TNF α , IL-1 β and IL-6 showed high specificity, which was confirmed by total lack of labeling in the negative control reaction. Immunoreactive cells showed a dark brown staining exclusively confined to the cytoplasm for TRAP (Fig. 6), and confined to the cytoplasm and to a lesser extent to the extracellular matrix for TNF α , IL-1 β and IL-6 (Fig. 7).

3.6. TRAP in bone tissue of tooth extraction site

TRAP immunolabeling was present in osteoclasts. The number of TRAP-positive cells per mm² and TRAP-positive cells per mm did not differ in ZOL and ZOL/aPDT groups. However, these parameters were lower when compared with VEH and VEH/aPDT groups (Fig. 6).

3.7. Immunolabeling for TNF α , IL-1 β and IL-6 in mucosal connective tissue overlying the tooth extraction site

Immunolabeling for TNF α , IL-1 β and IL-6 was present in inflammatory cells. The extracellular matrix of connective tissue also exhibited labeling ranging from mild to moderate. The immunolabeling

optical density for TNF α , IL-1 β and IL-6 was higher in ZOL and ZOL/aPDT groups than in VEH, except in ZOL/aPDT, where IL-1 β did not differ from VEH. The immunolabeling optical density for all the inflammatory cytokines was lower in ZOL/aPDT than in ZOL group (Fig. 7).

4. Discussion

In the present study, we employed an experimental model, which was established and characterized by our research group and designed based on epidemiological studies [5–7]. Such epidemiological studies have shown that BRONJ is most commonly observed in elderly women, which justifies the use of senile female rats (20 months old). We used zoledronate, as it is related to most cases of BRONJ, as well as adopted the dosage used to complement oncological therapy. Tooth extraction, especially of posterior lower teeth, and presence of periodontal disease are the first and second local risk factors for BRONJ, respectively [5–7]. Thus, experimental periodontitis was induced in the lower first molar tooth, following its extraction to mimic a very common clinical condition of patients at this age group, due to irreversible periodontal impairment.

Zoledronate alters bone metabolism by inhibiting the mevalonate pathway in osteoclasts, acting specifically on the farnesyl diphosphate synthase enzyme [31]. This action prevents changes to occur in the dynamics of the cytoskeleton, preventing the formation of the ruffled border and clear zone in the osteoclasts, which are essential for cell-bone matrix interaction and for the formation of the microenvironment favorable to the onset of the bone resorptive activity [31]. Furthermore, it inhibits osteoclastogenesis and induces premature apoptosis in active osteoclasts [32]. In this study, although only the tooth socket under repair process and its surroundings were the focus of analysis, the effects of zoledronate were also evident. In the groups treated with zoledronate, a smaller amount of TRAP-positive cells (expressed per mm² or per mm of vital bone tissue) were found when compared with the group treated with vehicle. In agreement with our findings, studies have shown that treatment with zoledronate is associated with a drastic reduction in both RANKL/OPG [33] and in TRAP 5b serum [33] in the tooth extraction site. Histologic and immunohistochemical analysis also revealed that the present osteoclasts showed characteristics of inactivity, that is, large rounded, hypernucleated cells, without cell polarization and distant from the bone matrix.

The actions of the zoledronate were not restricted to the osteoclasts only; other cells that participate in the tissue repair process, as well as the vasculature were affected by this drug [34–41]. In this study,

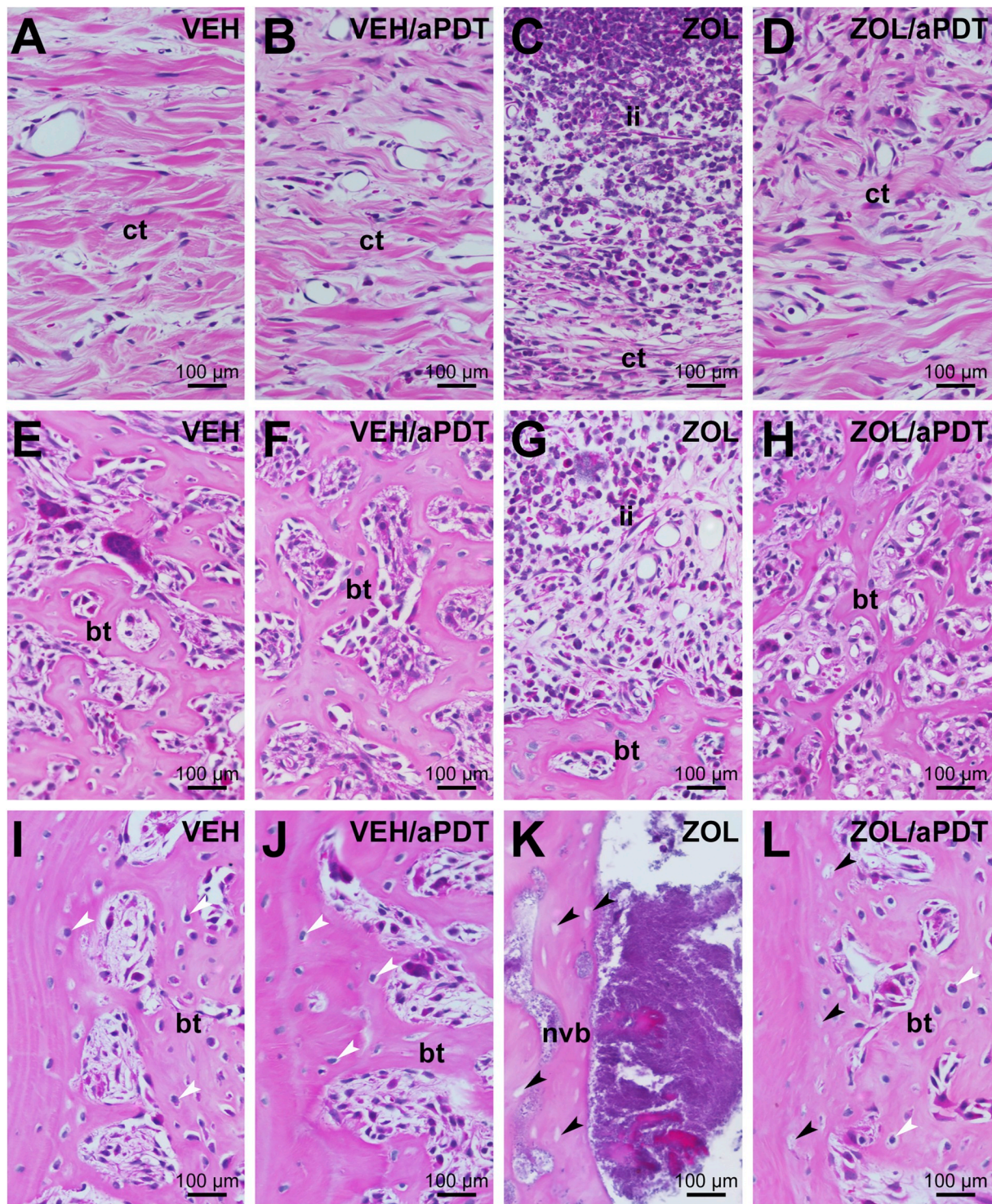


Fig. 2. Histological aspects of tooth extraction site and adjacent area. A–L: Photomicrographs showing histological characteristics of connective tissue and bone tissues in extraction site and adjacent area in VEH (A, E, I), VEH/aPDT (B, F, J), ZOL (C, G, K) and ZOL/aPDT (D, H, L) groups at 28 postoperative days. Observe in ZOL: persistence of inflammation in connective tissue overlying tooth extraction site (C, G); frequent presence of area occupied by non-vital bone (K). In VEH and ZOL/aPDT, histological characteristics were similar: absence of inflammation in connective tissue overlying tooth extraction site (A, D); absence of large areas of non-vital bone (E, H, I, L); presence of small quantity of empty lacunae (L) and; no bone sequestrum formation in adjacencies of extraction site. Abbreviations and symbols: bt, bone tissue; ct, connective tissue; nvb, non-vital bone; white arrows, osteocytes; black arrows, empty lacunae or occupied by necrotic remains of osteocytes. Staining: HE. Original magnification: 400 \times . Scale bars: 100 μ m.

zedronate impaired the repair of the soft tissue overlying the tooth extraction site. This bisphosphonate prevented reepithelialization and impaired connective tissue repair, causing persistent inflammation in the lamina propria and deconstructed of extracellular matrix with

negative inference on fibrillogenesis of collagen fibers. These results are in agreement with previous studies demonstrating that BPs exert a negative effect on keratinocytes and fibroblasts [34–38], which are cells that structure the epithelial and connective tissues, respectively. These

Table 2

Parameters, scores and distribution of specimens according to histological analysis during repair tissue after tooth extraction in VEH, VEH/aPDT, ZOL and ZOL/aPDT at 28 postoperative days.

Histological analysis	Number of specimens			
	Experimental groups			
	VEH (n = 7)	VEH/aPDT (n = 7)	ZOL (n = 7)	ZOL/aPDT (n = 7)
Parameters and respective scores				
Intensity of local inflammatory response				
(1) Absence of inflammation (presence of rare inflammatory cells)	7	7	–	5
(2) Small quantity of inflammatory cells (< 1/3 of cells are inflammatory cells)	–	–	–	2
(3) Moderate quantity of inflammatory cells (from 1/3–2/3 of cells are inflammatory cells)	–	–	3	–
(4) Large quantity of inflammatory cells (over 2/3 of cells are inflammatory cells)	–	–	4	–
Median	1	1	4 ^{†‡}	1
Inflammation extension				
(1) Absence of inflammation	7	7	–	5
(2) Partial extension of connective tissue	–	–	–	2
(3) Entire extension of connective tissue, without reaching bone tissue	–	–	2	–
(4) Entire extension of connective tissue and bone tissue	–	–	5	–
Median	1	1	4 ^{†‡}	1
Cellular pattern and epithelial tissue structure				
(1) epithelial tissue with moderate thickness (larger than half the surgical wound epithelium border thickness) and completely covering extraction site	4	6	–	2
(2) epithelial tissue with thin thickness (smaller than half the surgical wound epithelium border thickness) and completely covering extraction site	3	1	–	5
(3) thin layer of epithelial tissue (smaller than half the surgical wound epithelium border thickness) and only in edges of open surgical wound	–	–	4	–
(4) absence of epithelial tissue and open surgical wound	–	–	3	–
median	1	1	3 ^{†‡}	2 [¶]
cellular pattern and connective tissue structure				
(1) Moderate quantity of fibroblasts and large quantity of collagen fibers (approximately 2/3 of area occupied by fibroblasts/collagen fibers, where collagen fibers are prevalent over fibroblasts)	4	6	–	3
(2) Moderate quantity of both fibroblasts and collagen fibers (approximately 2/3 of area occupied by fibroblasts/collagen fibers, where collagen fibers and fibroblasts are equivalent)	3	1	–	4
(3) Small quantity of both fibroblasts and collagen fibers (approximately 1/3 of area occupied by fibroblasts/collagen fibers, where collagen fibers and fibroblasts are equivalent)	–	–	2	–
(4) Severe tissue disorganization with necrosis areas (approximately 2/3 of area occupied by disorganized connective tissue)	–	–	5	–
Median	1	1	4 ^{†‡}	2 [¶]
Cellular pattern and bone tissue structure				
(1) Absence of non-vital bone in adjacencies of extraction site and trabecular bone filling more than half of tooth socket	6	7	–	5
(2) Absence of non-vital bone in adjacencies of extraction site and trabecular bone filling less than half of tooth socket	1	–	–	2
(3) Presence of few areas with non-vital bone in adjacencies of extraction site and trabecular bone filling less than a third of tooth socket	–	–	2	–
(4) Presence of many areas with non-vital bone in adjacencies of extraction site and trabecular bone filling less than a third of tooth socket	–	–	5	–
median	1	1	4 ^{†‡}	2 [¶]
Contamination pattern of tooth extraction site				
(1) Presence of small quantity bacteria diffusely distributed in tooth extraction site, typical of a normal condition	7	7	–	6
(2) Presence of large colonies of bacteria in soft tissues over tooth socket	–	–	–	1
(3) Presence of large colonies of bacteria in surface of alveolar bone and in the interior of the tooth socket	–	–	–	1
(4) Presence of large colonies of bacteria involving necrosed bone and/or in medullar spaces and in adjacencies of tooth socket	–	–	7	–
median	1	1	4 ^{†‡}	2 [¶]

Symbols: †, statistically significant difference in relation to VEH; ‡, statistically significant difference in relation to VEH/aPDT; ¶, statistically significant difference in relation to ZOL.

studies showed that BPs are capable of decreasing proliferation and increasing the occurrence of apoptosis in keratinocytes [34–36] and fibroblasts [37,38] of the oral mucosa. Another aspect that should be highlighted is the involvement of high levels of pro-inflammatory cytokines with the etiopathogenesis of BRONJ. Morita et al. [42] reported that TNF α -, IL-1 β - and IL-6- deficient mice were resistant to osteonecrosis development. These authors showed that among the sources of proinflammatory cytokines are the osteoclast precursors, whose maturation was inhibited by the use of BPs [42].

The histological and histometric analyses performed in the present study demonstrated that zoledronate impaired the alveolar bone healing process after tooth extraction. In group ZOL, an extremely low amount of NFBT, indicating a negative effect of zoledronate on bone-

forming cells was observed at 28 postoperative days after tooth extraction. Corroborating our findings, some studies have also shown that zoledronate negatively affects pre-osteoblasts and osteoblasts [39–41]. Huang et al. [43] reported that zoledronate exerts potent cytotoxic effects on osteoblasts at high concentrations, but affects the differentiation process of their precursors at low concentrations. These authors also showed that bone morphogenetic protein 2, alkaline phosphatase and osteocalcin gene expression suffer dose-dependent reduction on osteoblasts treated with zoledronate. Furthermore, in this group, a large amount of NVTB was found, which comprised both areas of alveolar bone still structured but devoid of osteocytes in lacunae as well as large bony sequestrum enclosed by bacteria, inflammatory cells and necrotic debris. These data can be explained by a cytotoxic effect on osteocytes

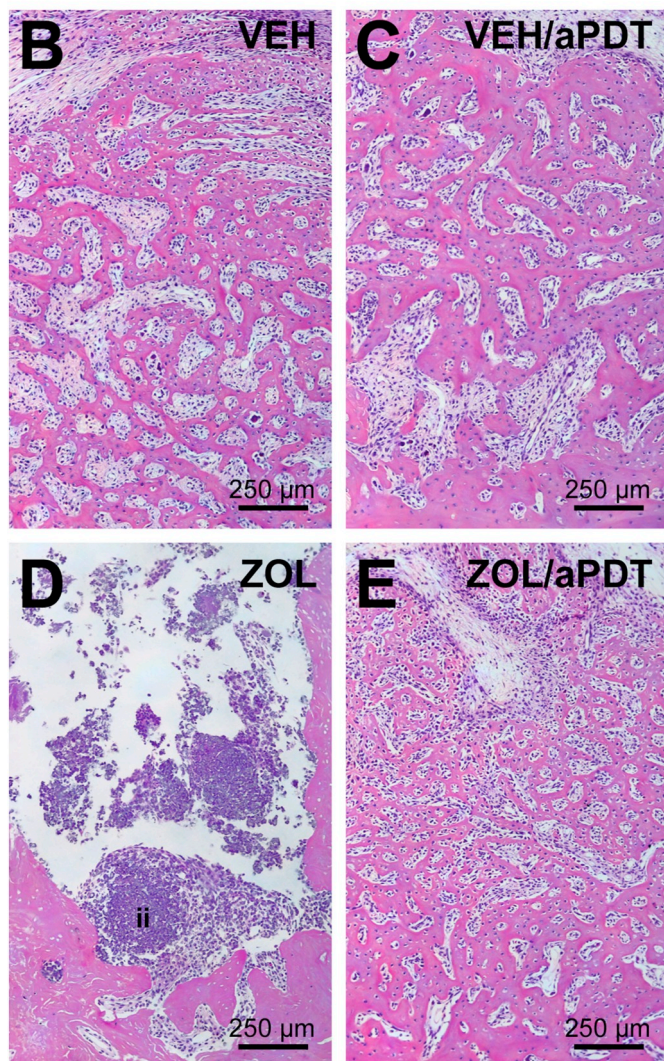
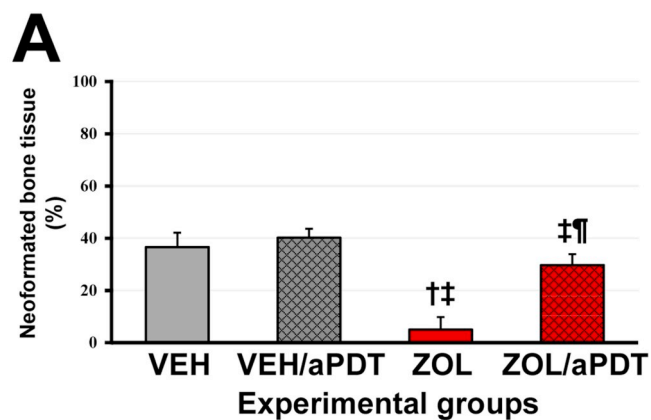


Fig. 3. Newly formed bone in tooth extraction site. A: percentage of newly formed bone tissue (NFBT) in extraction site in the different experimental groups at 28 postoperative days. B-E: Photomicrographs showing percentage of NFBT in extraction site previously occupied by mesial root of first molar in groups VEH (B), VEH/aPDT (C), ZOL (D) and ZOL/aPDT (E). Abbreviations and symbols: ii, inflammatory infiltrate; †, statistically significant difference in relation to VEH; ‡, statistically significant difference in relation to VEH/aPDT; ¶, statistically significant difference in relation to ZOL. Staining: HE. Original magnification: 100×. Scale bars: 250 μm.

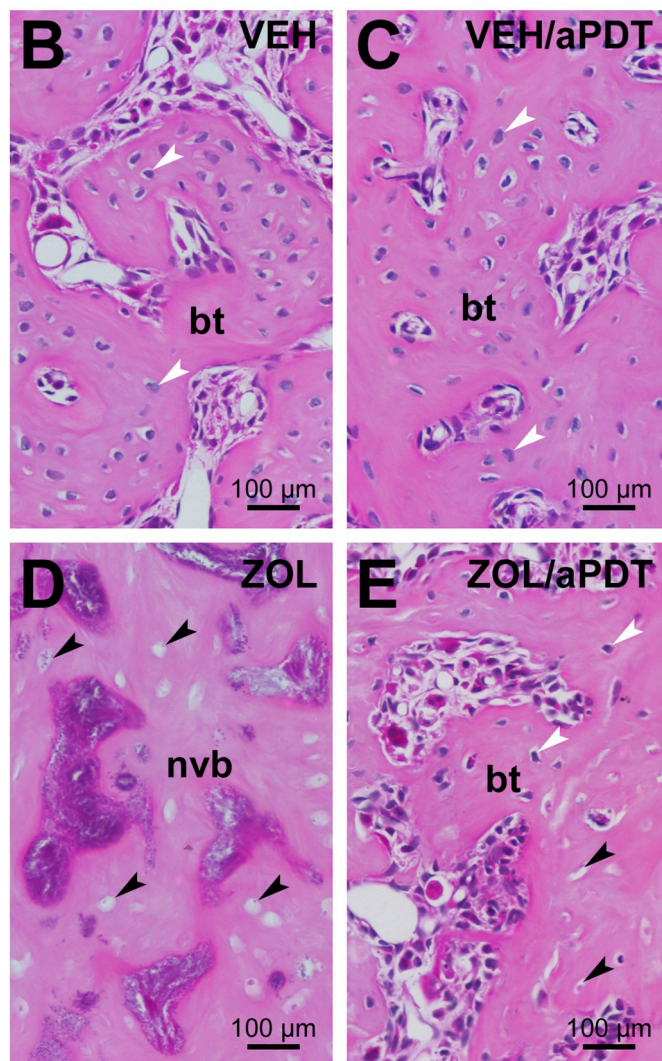
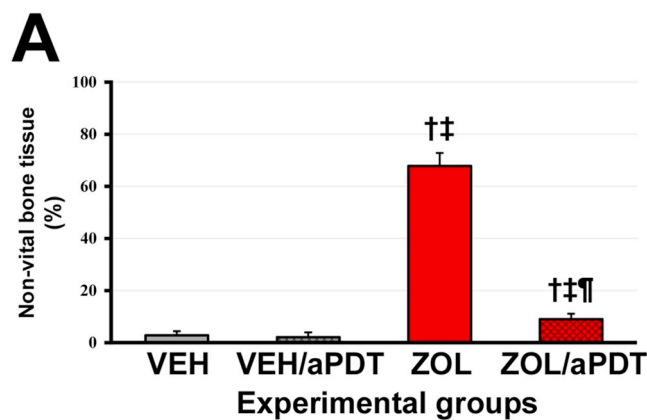


Fig. 4. Vital and non-vital bone tissue in areas adjacent to tooth extraction site. A: percentage of non-vital bone tissue (NVBT) in areas adjacent to extraction site in the different experimental groups at 28 postoperative days. B-E: Photomicrographs showing different amounts of vital and non-vital bone tissue in areas adjacent to extraction site in groups VEH (B), VEH/aPDT (C), ZOL (D) and ZOL/aPDT (E). Abbreviations and symbols: nvb, non-vital bone; white arrows, osteocytes; black arrows, empty lacunae or occupied by necrotic remains of osteocytes; †, statistically significant difference in relation to VEH; ‡, statistically significant difference in relation to VEH/aPDT; ¶, statistically significant difference in relation to ZOL. Staining: HE. Original magnification: 100×. Scale bars: 250 μm.

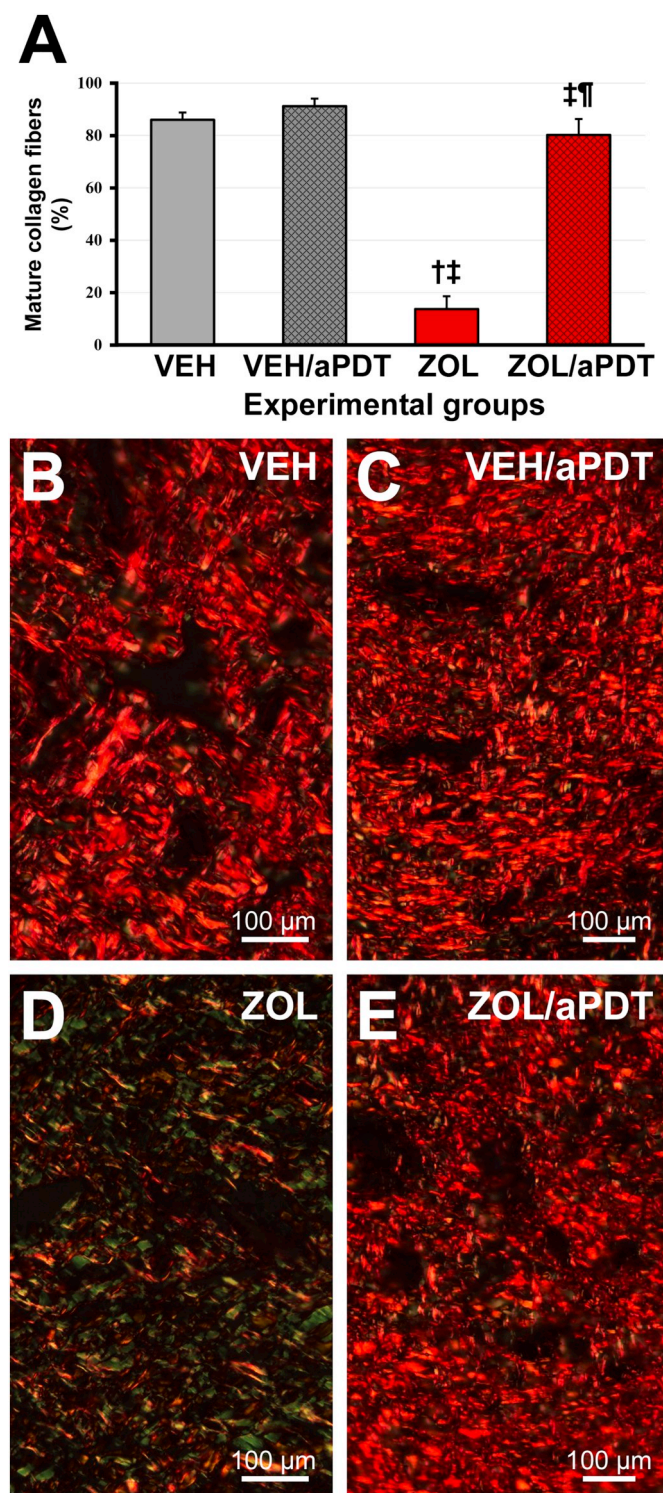


Fig. 5. Maturation level of collagen fibers in tooth extraction site. **A:** percentage of mature collagen fibers in connective tissue of mucous membrane overlying extraction site in the different experimental groups at 28 postoperative days. **B–E:** Photomicrographs showing maturation pattern of collagen fibers in VEH (**B**), VEH/aPDT (**C**), ZOL (**D**) and ZOL/aPDT (**E**). Symbols: †, statistically significant difference in relation to VEH; ‡, statistically significant difference in relation to VEH/aPDT; ¶, statistically significant difference in relation to ZOL. Staining: picosirius red under polarized light microscopy. Original magnification: 250 \times . Scale bars: 100 μ m. (For interpretation of the references to color in this figure legend, the reader is referred to the web version of this article.)

or by non-vital bone tissue buildup due to the suppression of osteoclast resorptive activity, especially after tooth extraction, which is a traumatic procedure. Other studies in similar experimental models showed that zoledronate significantly increases the amount of non-vital bone tissue [28,44–45].

In the present study, we confirmed our hypothesis that the use of multiple aPDT sessions in the tooth extraction site of female rats treated with zoledronate improved the alveolar repair process and prevented the occurrence of BRONJ-like lesions. Successful aPDT depend on the photosensitizer (type and concentration), on the irradiation parameters (wavelength and power), on the phototherapy protocol (exposure time and released energy) and on the local microbiota [26]. The photosensitizer employed in the present study was methylene blue (100 μ g/ml), a phenothiazine that presents maximum irradiation absorption at wavelength of 660 nm. The choice of this photosensitizer, the pre-irradiation exposure time and concentration were based on a previous study performed by our research team [26]. The irradiation parameters (660 nm; 35 mW; 2.1 J/point; 60 s; 74.2 J/cm²) were adapted for reaching maximum photosensitizer activity on the microbial cells that absorbed it, and for reaching a photobiomodulatory effect on the cells of the host that did not absorb it [26]. Besides, aPDT employing methylene blue with low-level laser irradiation has proven extremely effective against several microorganisms, including common buccal cavity bacteria [46].

The present study observed that the use of aPDT in the tooth extraction site of senile female rats treated with zoledronate was not able to alter the number of osteoclasts (expressed per mm² or per mm of vital bone tissue). Thus, the local therapy did not influence the systemic effect of zoledronate on such cells. Osteoclasts are cells that participate in the alveolar repair process [47]. Moreover, the suppression of bone resorption is considered a putative etiopathogenic factor of BRONJ-like lesions; however, in ZOL/aPDT group the inhibition of its activity did not significantly interfere in this process. Supposedly, the aPDT biomodulation activity on other cell types, such as keratinocytes, fibroblasts and osteoclasts, and on the vasculature have resulted in improvement of the tissue repair process [18,19], even without the effective participation of osteoclasts in this process.

The photobiomodulatory action of the low-level laser employed in the aPDT has cytochrome c oxidase in the complex IV of the mitochondrial respiratory chain as main targets [18,19]. Such chromophore acts as a photoreceptor and transducer of photsignals and its stimulation promotes an increase of adenosine triphosphate (ATP), cyclic adenosine monophosphate (cAMP), nitric oxide (NO) and ROS [18,19]. Another important target of the low-level laser is the light sensitive ionic channels that can be activated, allowing calcium influx in the cell [18,19]. Following the initial events of photon absorption, several signaling pathways are activated leading to the induction of different transcription factors. Such transcription factors trigger specific gene expressions involved in proliferation, migration and cellular differentiation, increase cell metabolic activity, as well as trigger the activation of signaling pathways that modulate angiogenesis, inflammatory response and cellular apoptosis, and increase antioxidant enzyme levels [18,19], events involved with the alveolar repair process.

The histological characteristics of the epithelium, lamina propria, structuring of collagen fibers and the decrease in immunolabeling for the main pro-inflammatory cytokines in the mucosa overlying the tooth extraction site in ZOL/aPDT group showed that aPDT was able to reverse the negative effects of zoledronate. This study was the first to propose and characterize aPDT as a preventive strategy to avoid BRONJ in face of the main risk factors for the disease. Our findings are in agreement with studies performed in other soft tissues showing that aPDT had a positive effect on the repair process of epithelial and connective tissues and reduced local infection. Studies in infected cutaneous wounds showed that aPDT reduced the bacterial load [48], decreased inflammation [48–50], and exerted a stimulatory effect on neoangiogenesis [50], cell proliferation [50], reepithelialization rate

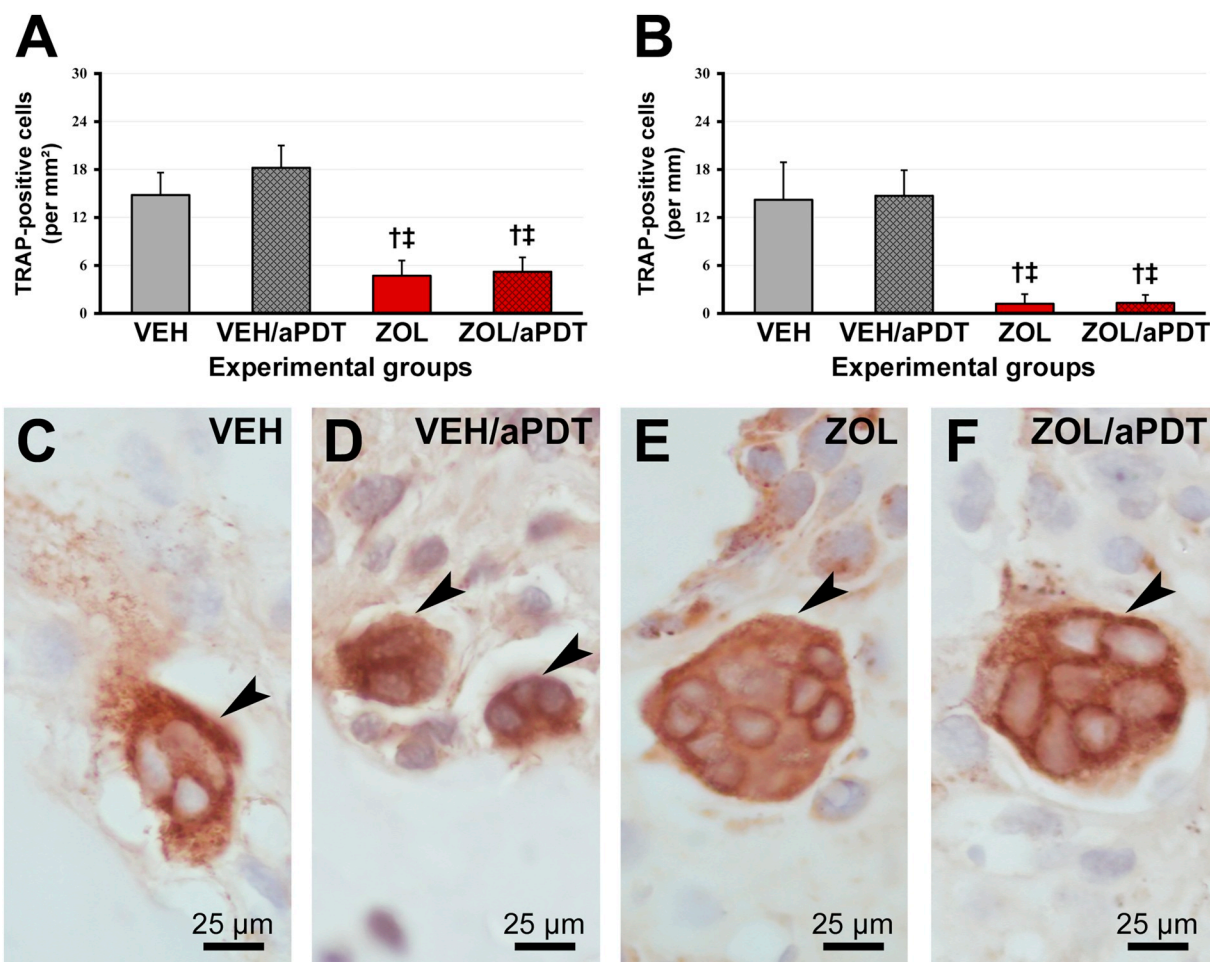


Fig. 6. Immunolabeling pattern for TRAP in tooth extraction site. A–B: immunolabeling data for TRAP-positive cells per mm² (A) and TRAP-positive cells per mm (B) in vital tissue bone of tooth extraction site in the different experimental groups at 28 postoperative days. C–F: Photomicrographs showing TRAP-positive cells in VEH (C), VEH/aPDT (D), ZOL (E) and ZOL/aPDT (F). Symbols: arrows, osteoclasts; †, statistically significant difference in relation to VEH; ‡, statistically significant difference in relation to VEH/aPDT. Original magnification: 2000 \times . Scale bars: 25 μ m.

[48–51] and extracellular matrix remodeling [51]. Likewise, the use of aPDT in third degree skin burn stimulated the tissue repair process both in the epidermis and dermis layers [52]. Moreover, it has been reported that aPDT reduced the severity of oral mucositis induced by 5-fluorouracil [53].

No previous studies used aPDT as a preventative therapeutic strategy to avoid BRONJ post tooth extraction. However, the use of this therapy in other infectious/inflammatory conditions involving simultaneous healing process of soft tissue and alveolar bone tissue has achieved satisfactory results. This treatment modality has been successfully adopted to promote tissue repair of infected dental extraction wounds [54]. Furthermore, aPDT has proven an effective therapy when used in association with root planing and scaling in the treatment of experimental periodontitis, another infectious/inflammatory condition [55]. The positive effects of aPDT in the periodontal repair process were reported even in situations where the host response had some type of commitment, such as diabetes [56], severe immunosuppression [57], nicotine action [58,59] or depletion of sex hormones in females [58]. aPDT, even when employed as a monotherapy, exerted beneficial effects on the periodontal healing of rats with experimental periodontitis and undergoing chemotherapy with 5-fluorouracil [60].

Although BRONJ and osteomyelitis do not exhibit similar pathophysiology, they have similar clinical features, which allow us to establish some correlations between them. Studies in an experimental model of osteomyelitis induced via surgical bone defects in the tibia and contamination with *Staphylococcus aureus*, showed positive aPDT

effects, reducing the microbial load and allowing the continuity of the tissue repair process [61,62]. Considering these studies, it was found that when used in the treatment of infected bone lesions, aPDT is effective in controlling infection and promoting tissue repair. The findings of the present study showed that when used preventively, i.e., before larger osteonecrotic lesions are established, aPDT concomitantly stimulated tissue repair process and prevented the occurrence of infection. Although infection follows most cases of BRONJ, we believe this is a secondary event resulting from a severe impairment of the tissue repair process, which would explain failure of the antibiotic therapy.

The antimicrobial activity of aPDT is of fundamental importance to favor the repair process. The combination of PS pre-absorbed by microbial cells, light with a suitable wavelength and oxygen generates high levels of ROS which are highly cytotoxic to the microbial cells which leads to the death of such cells and avoiding infection [16,17]. Although this study did not focus on an accurate microbiological evaluation, it is worth highlighting that while ZOL group had areas of necrotic bone surrounded by colonies of bacteria; the same was not observed in ZOL/aPDT group, demonstrating an antimicrobial action. Hallmer, et al. [63] reported eight dominating bacteria groups on bone samples from BRONJ patients: *Porphyromonas*, *Lactobacillus*, *Tannerella*, *Prevotella*, *Actinomyces*, *Treponema*, *Streptococcus*, and *Fusobacterium*. A study in an experimental model of BRONJ-like lesions evidenced an important association with *Fusobacterium* [64]. Other studies reported a strong correlation between BRONJ and *Actinomyces* [65–67].

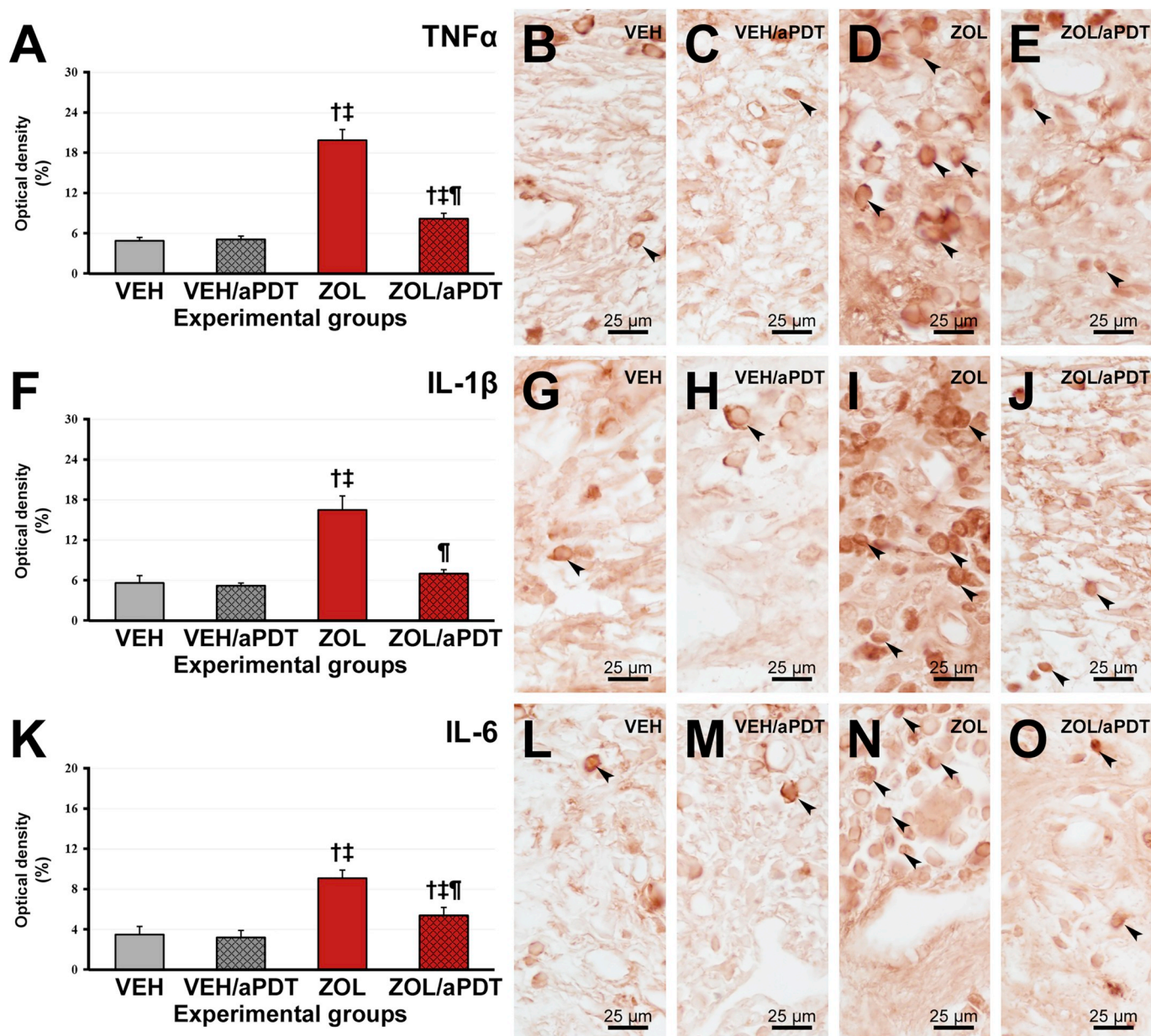


Fig. 7. Immunolabeling pattern for TNF α , IL-1 β and IL-6 in tooth extraction site. A, F, K: immunolabeling data for TNF α (A), IL-1 β (F) and IL-6 (K) in tissue of extraction site in the different experimental groups at 28 postoperative days. B–E, G–J and L–O: Photomicrographs showing immunolabeling pattern for TNF α (B–E), IL-1 β (G–J) and IL-6 (L–O) in VEH (B, G, L), VEH/aPDT (C, H, M), ZOL (D, I, N) and ZOL/aPDT (E, J, O). Symbols: †, statistically significant difference in relation to VEH; ‡, statistically significant difference in relation to VEH/aPDT; ¶, statistically significant difference in relation to ZOL. Original magnification: 1000 \times . Scale bars: 25 μ m.

Theodoro et al. [21] showed that aPDT is an effective treatment to reduce the microbial load of dental alveolus post-molar extraction with experimental periodontitis. Hafner et al. [68] reported in an in vitro study that aPDT promoted a four-fold reduction in the bacterial load of *Actinomyces naeslundii* isolated from patients with BRONJ, when compared with chlorhexidine and polyhexanide treatments. The data from this study support that aPDT had an antimicrobial action in the tooth extraction site of rats treated with zoledronate. However, further microbiological studies are required to support these findings.

BRONJ and its treatment significantly affect the quality of life of patients. In some cases, the treatment may prove flawed or result in serious consequences. In view of this, the use of preventive therapeutic strategies would be ideal in the case of BRONJ. The findings of this study may be important to guide future clinical research. Clinical studies for the establishment of preventive protocols to be used in patients

who make use of antiresorptive drugs and require invasive dental interventions are needed. The aPDT may constitute a promising preventive therapy considering its antimicrobial action, potent biomodulatory activity and no adverse side effects.

5. Conclusion

Within the limits of this study, it was concluded that the use of multiple aPDT sessions in the tooth extraction site improves alveolar repair process and prevents the occurrence of BRONJ-like lesions after tooth extraction in senile female rats treated with zoledronate.

Acknowledgements

The authors would like to thank the São Paulo Research Foundation

(FAPESP - Process # 2012/03067-6; # 2013/26779-4; # 2013/25367-4; # 2014/02199-1; # 2015/22395-2) and the National Council for Scientific and Technological Development (CNPq - Process # 30699-2014; # 28040-2013) for the research grant and financial support to conduct this study.

Declarations of interest

None.

Author contributions

EE, conceptualization of study, supervision of data collection; supervision of data analysis, data validation, data discussion, manuscript preparation and revision, funding acquisition and project administration; CS, LFT, JMMN and TPC, execution of experimental procedures, data collection and analysis, data discussion and manuscript preparation; JPMI, RCMD, JMA, RO, MJHN and CAC, data validation, data discussion, manuscript revision; VGG and LHT, conceptualization of study, data validation, data discussion, manuscript preparation and revision.

References

- I.S. Hamadeh, B.A. Ngwa, Y. Gong, Drug induced osteonecrosis of the jaw, *Cancer Treat. Rev.* 41 (2015) 455–464.
- M.T. Drake, B.L. Clarke, S. Khosla, Bisphosphonates: mechanism of action and role in clinical practice, *Mayo Clin. Proc.* 83 (9) (2008) 1032–1045.
- R.E. Marx, Pamidronate (Aredia) and zoledronate (Zometa) induced avascular necrosis of the jaws: a growing epidemic, *J. Oral Maxillofac. Surg.* 61 (2003) 115–117.
- S.L. Ruggiero, T.B. Dodson, American association of oral and maxillofacial surgeons position paper on medication-related osteonecrosis of the jaws - 2014 update, *J. Oral Maxillofac. Surg.* 72 (2014) 2381–2382.
- A.A. Khan, A. Morrison, D.L. Kendler, R. Rizzoli, D.A. Hanley, D. Felsenberg, L.K. McCauley, F. O'ryan, I.R. Reid, S.L. Ruggiero, A. Taguchi, S. Tetradis, N.B. Watts, M.L. Brandi, E. Peters, T. Guise, R. Eastell, A.M. Cheung, S.N. Morin, B. Masri, C. Cooper, S.L. Morgan, B. Obermayer-Pietsch, B.L. Langdahl, R.A. Dabagh, K.S. Davison, G.K. Sándor, R.G. Josse, M. Bhandari, M. El Rabbany, D.D. Pierroz, R. Sulimani, D.P. Saunders, J.P. Brown, J. Compston, International Task Force on Osteonecrosis Of The Jaw, Case-based review of osteonecrosis of the jaw (ONJ) and application of the international recommendations for management from the international task force on ONJ, *J. Clin. Densitom.* 20 (2017) 8–24.
- K. McGowan, T. McGowan, S. Ivanovski, Risk factors for medication-related osteonecrosis of the jaws: a systematic review, *Oral Dis.* 24 (2018) 527–536 (Epub ahead of print).
- S. Otto, C. Schreyer, S. Hafner, G. Mast, M. Ehrenfeld, S. Stürzenbaum, C. Pautke, Bisphosphonate-related osteonecrosis of the jaws - characteristics, risk factors, clinical features, localization and impact on oncological treatment, *J. Craniomaxillofac. Surg.* 40 (2012) 303–309.
- T. Aghaloo, R. Hazboun, S. Tetradis, Pathophysiology of osteonecrosis of the jaws, *Oral Maxillofac. Surg. Clin. North Am.* 27 (2015) 489–496.
- T. Badel, I.S. Pavicin, A.J. Carek, K. Rosin-Grget, D. Grbesa, Pathophysiology of osteonecrosis of the jaw in patients treated with bisphosphonate, *Coll. Antropol.* 37 (2013) 645–651.
- C.A. Migliorati, J.B. Epstein, E. Abt, J.R. Berenson, Osteonecrosis of the jaw and bisphosphonates in cancer: a narrative review, *Nat. Rev. Endocrinol.* 7 (2011) 34–42.
- M.R. Allen, D.B. Burr, The pathogenesis of bisphosphonate-related osteonecrosis of the jaw: so many hypotheses, so few data, *J. Oral Maxillofac. Surg.* 67 (5 Suppl) (2009) 61–70.
- M. El-Rabbany, A. Sgro, D.K. Lam, P.S. Shah, A. Azarpazhooh, Effectiveness of treatments for medication-related osteonecrosis of the jaw: a systematic review and meta-analysis, *J. Am. Dent. Assoc.* S0002-8177 (2017) 30300–30308.
- S. Hayashida, S. Soutome, S. Yanamoto, S. Fujita, T. Hasegawa, T. Komori, Y. Kojima, H. Miyamoto, Y. Shibuya, N. Ueda, T. Kirita, H. Nakahara, M. Shinohara, M. Umeda, Evaluation of the treatment strategies for medication-related osteonecrosis of the jaws (MRONJ) and the factors affecting treatment outcome: a multicenter retrospective study with propensity score matching analysis, *J. Bone Miner. Res.* 32 (2017) 2022–2029.
- A. Khan, A. Morrison, A. Cheung, W. Hashem, J. Compston, Osteonecrosis of the jaw (ONJ): diagnosis and management in 2015, *Osteoporos. Int.* 27 (2016) 853–859.
- S. Hoefert, H. Eufinger, Relevance of a prolonged preoperative antibiotic regime in the treatment of bisphosphonate-related osteonecrosis of the jaw, *J. Oral Maxillofac. Surg.* 69 (2) (2011) 362–380.
- E.T. Carrera, H.B. Dias, S.C.T. Corbi, R.A.C. Marcantonio, A.C.A. Bernardi, V.S. Bagnato, M.R. Hamblin, A.N.S. Rastelli, The application of antimicrobial photodynamic therapy (aPDT) in dentistry: a critical review, *Laser Phys.* 26 (12) (2016) p.pii:123001.
- M. Wainwright, T. Maisch, S. Nonell, K. Plaetzer, A. Almeida, G.P. Tegos, M.R. Hamblin, Photoantimicrobials-are we afraid of the light? *Lancet Infect. Dis.* 17 (2) (2017) e49–e55.
- L.F. De Freitas, M.R. Hamblin, Proposed mechanisms of photobiomodulation or low-level light therapy, *IEEE J. Sel. Top. Quantum Electron.* 22 (3) (2016) p.pii:7000417.
- P.R. Arany, Craniofacial wound healing with photobiomodulation therapy: new insights and current challenges, *J. Dent. Res.* 95 (9) (2016) 977–984.
- C. Statkiewicz, L.F. Toro, J.M. Mello-Neto, D.P. Sá, C.A. Casatti, J.P.M. Issa, L.T.A. Cintra, J.M. Almeida, M.J.H. Nagata, V.G. Garcia, L.H. Theodoro, E. Ervolino, Photomodulation multiple sessions as a promising preventive therapy for medication-related osteonecrosis of the jaws after tooth extraction in rats, *J. Photochem. Photobiol. B* 184 (2018) 7–17.
- L.H. Theodoro, J.R. Pires, L.A. Fernandes, E.C. Gualberto Júnior, M. Longo, J.M. De Almeida, V.G. Garcia, Effect of antimicrobial photodynamic therapy on periodontally infected tooth sockets in rats, *Lasers Med. Sci.* 30 (3) (2015) 677–683.
- G. Batinjan, Z. Zore, A. Čelebić, M. Papić, D. Gabrić Pandurić, I. Filipović Zore, Thermographic monitoring of wound healing and oral health-related quality of life in patients treated with laser (aPDT) after impacted mandibular third molar removal, *Int. J. Oral Maxillofac. Surg.* 43 (2014) 1503–1508.
- G. Batinjan, I. Filipović Zore, I. Rupić, I. Bago Jurić, Z. Zore, D. Gabrić Pandurić, Assessing health-related quality of life with antimicrobial photodynamic therapy (APDT) and low level laser therapy (LLLT) after third molar removal, *J. Lasers Med. Sci.* 4 (2013) 120–126.
- J. Neugebauer, M. Jozsa, A. Kübler, Antimicrobial photodynamic therapy for prevention of alveolar osteitis and post-extraction pain, *Mund Kiefer Gesichtschir.* 8 (2004) 350–355.
- P.G. Silva, A.E. Ferreira Junior, C.R. Teófilo, M.C. Barbosa, R.C. Lima Júnior, F.B. Sousa, M.R. Mota, R.A. Ribeiro, A.P. Alves, Effect of different doses of zoledronic acid in establishing of bisphosphonate related osteonecrosis, *Arch. Oral Biol.* 60 (2015) 1237–1245.
- V.G. Garcia, M. Longo, E.C. Gualberto Júnior, A.F. Bosco, M.J.H. Nagata, E. Ervolino, L.H. Theodoro, Effect of the concentration of phenothiazine photosensitizers in antimicrobial photodynamic therapy on bone loss and the immune inflammatory response of induced periodontitis in rats, *J. Periodontol. Res.* 49 (2014) 584–594.
- R. Latouf, R. Younes, D. Lutowski, N. Naaman, G. Godeau, K. Senni, S. Changotade, Picrosirius red staining: a useful tool to appraise collagen networks in normal and pathological tissues, *J. Histochem. Cytochem.* 62 (10) (2014) 751–758.
- S.J.R. Martelli, M.F. Damian, A.P.N. Gomes, A.R. Schinestck, A.E.R. Silva, A.C.U. Vasconcelos, Comparison of effects of zoledronic acid and clodronate on the bone structure: imaginological and histomorphometrical study in vivo, *J. Oral Pathol. Med.* 46 (2017) 632–636.
- P.G.B. Coelho, M.V. Souza, L.G. Conceição, M.I.V. Vitoria, S.A.O. Bedoya, Evaluation of dermal collagen stained with picrosirius red and examined under polarized light microscopy, *An. Bras. Dermatol.* 93 (2018) 415–418.
- T.W. King, E.M. Brey, A.A. Youssef, C. Johnston, C.W. Patrick Jr, Quantification of vascular density using a semiautomated technique for immunostained specimens, *Anal. Quant. Cytol. Histol.* 24 (2002) 39–48.
- D.B. Kimmel, Mechanism of action, pharmacokinetic and pharmacodynamic profile, and clinical applications of nitrogen-containing bisphosphonates - review, *J. Dent. Res.* 86 (11) (2007) 1022–1033.
- K. Abe, Y. Yoshimura, Y. Deyama, T. Kikuri, T. Hasegawa, K. Tei, H. Shinoda, K. Suzuki, Y. Kitagawa, Effects of bisphosphonates on osteoclastogenesis in RAW264.7 cells, *Int. J. Mol. Med.* 29 (2012) 1007–1015.
- J.W. Kim, I.H. Cha, S.J. Kim, M.R. Kim, Biomarkers for bisphosphonate-related osteonecrosis of the jaw, *Clin. Implant. Dent. Relat. Res.* 18 (2) (2016) 281–291.
- A.M. Pabst, T. Ziebart, F.P. Koch, K.Y. Taylor, B. Al-Nawas, C. Walter, The influence of bisphosphonates on viability, migration, and apoptosis of human oral keratinocytes-in vitro study, *Clin. Oral Investig.* 16 (2012) 87–93.
- S. Saracino, R.A. Canuto, M. Maggiora, M. Oraldi, M. Scoletta, L. Ciuffreda, Exposing human epithelial cells to zoledronic acid can mediate osteonecrosis of jaw: an in vitro model, *J. Oral Pathol. Med.* 41 (2012) 788–792.
- M.A. Scheper, A. Badros, R. Chaisuparat, K.J. Cullen, T.F. Meiller, Effect of zoledronic acid on oral fibroblasts and epithelial cells: a potential mechanism of bisphosphonate-associated osteonecrosis, *Br. J. Haematol.* 144 (2009) 667–676.
- C. Walter, A. Pabst, T. Ziebart, M. Klein, B. Al-Nawas, Bisphosphonates affect migration ability and cell viability of HUVEC, fibroblasts and osteoblasts in vitro, *Oral Dis.* 17 (2011) 194–199.
- M.A. Scheper, A. Badros, R. Chaisuparat, K.J. Cullen, T.F. Meiller, Effect of zoledronic acid on oral fibroblasts and epithelial cells: a potential mechanism of bisphosphonate-associated osteonecrosis, *Br. J. Haematol.* 144 (2009) 667–676.
- L.A. Córdova, F. Guilbaud, J. Amiaud, S. Battaglia, C. Charrier, F. Lezot, B. Piot, F. Redini, D. Heymann, Severe compromise of preosteoblasts in a surgical mouse model of bisphosphonate-associated osteonecrosis of the jaw, *J. Craniomaxillofac. Surg.* 9 (2016) 1387–1394.
- F.G. Basso, A.P. Silveira Turroni, J. Hebling, C.A. De Souza Costa, Zoledronic acid inhibits human osteoblast activities, *Gerontology* 59 (2013) 534–541.
- A. Naidu, P.C. Dechow, R. Spears, J.M. Wright, H.P. Kessler, L.A. Opperman, The effects of bisphosphonates on osteoblasts in vitro, *Oral Surg. Oral Med. Oral Pathol. Oral Radiol. Endod.* 106 (2008) 5–13.
- M. Morita, R. Iwasaki, Y. Sato, T. Kobayashi, R. Watanabe, T. Oike, S. Nakamura, Y. Keneko, K. Miyamoto, K. Ishihara, Y. Iwakura, C. Ishii, M. Matsumoto, M. Nakamura, H. Kawana, T. Nakagawa, T. Miyamoto, Elevation of pro-inflammatory cytokine levels following anti-resorptive drug treatment is required for

- osteonecrosis development in infectious osteomyelitis, *Sci. Rep.* 7 (2017) 46322.
- [43] X. Huang, S. Huang, F. Guo, F. Xu, P. Cheng, Y. Ye, Y. Dong, W. Xiang, A. Chen, Dose-dependent inhibitory effects of zoledronic acid on osteoblast viability and function in vitro, *Mol. Med. Rep.* 13 (2016) 613–622.
- [44] M.L. Silva, L. Tasso, A.A. Azambuja, M.A. Figueiredo, F.G. Salum, V.D. Da Silva, K. Cherubini, Effect of hyperbaric oxygen therapy on tooth extraction sites in rats subjected to bisphosphonate therapy-histomorphometric and immunohistochemical analysis, *Clin. Oral Investig.* 21 (2017) 199–210.
- [45] A.C. Vasconcelos, S.A. Berti-Couto, A.A. Azambuja, F.G. Salum, M.A. Figueiredo, V.D. Da Silva, K. Cherubini, Comparison of effects of clodronate and zoledronic acid on the repair of maxilla surgical wounds - histomorphometric, receptor activator of nuclear factor- κ B ligand, osteoprotegerin, von Willebrand factor, and caspase-3 evaluation, *J. Oral Pathol. Med.* 41 (2012) 702–712.
- [46] F.F. Sperandio, Y.Y. Huang, M.R. Hamblin, Antimicrobial photodynamic therapy to kill gram-negative bacteria, *Recent Pat. Anticancer Drug Discov.* 8 (2) (2013) 108–120.
- [47] E.R. Luvizuto, S.S. Dias, T. Okamoto, R.C. Dornelles, R. Okamoto, Raloxifene therapy inhibits osteoclastogenesis during the alveolar healing process in rats, *Arch. Oral Biol.* 56 (10) (2011) 984–990.
- [48] K. Sahu, M. Sharma, H. Bansal, A. Dube, P.K. Gupta, Topical photodynamic treatment with poly-L-lysine-chlorin p6 conjugate improves wound healing by reducing hyperinflammatory response in *Pseudomonas aeruginosa*-infected wounds of mice, *Lasers Med. Sci.* 28 (2013) 465–471.
- [49] K. Sahu, M. Sharma, P.K. Gupta, Modulation of inflammatory response of wounds by antimicrobial photodynamic therapy, *Laser Ther.* 24 (2015) 201–208.
- [50] K. Sahu, M. Sharma, A. Dube, P.K. Gupta, Topical antimicrobial photodynamic therapy improves angiogenesis in wounds of diabetic mice, *Lasers Med. Sci.* 30 (2015) 1923–1929.
- [51] K. Sahu, M. Sharma, P. Sharma, Y. Verma, K.D. Rao, H. Bansal, A. Dube, P.K. Gupta, Effect of poly-L-lysine-chlorin P6-mediated antimicrobial photodynamic treatment on collagen restoration in bacteria-infected wounds, *Photomed. Laser Surg.* 32 (2014) 23–29.
- [52] V.G. Garcia, M.A. De Lima, T. Okamoto, L.A. Milanezi, E.C. Júnior, L.A. Fernandes, J.M. De Almeida, L.H. Theodoro, Effect of photodynamic therapy on the healing of cutaneous third-degree-burn: histological study in rats, *Lasers Med. Sci.* 25 (2010) 221–228.
- [53] P. Cruz Éde, L. Campos, F.D.A.S. Pereira, G.C. Magliano, B.M. Benites, V.E. Arana-Chavez, R.Y. Ballester, A. Simões, Clinical, biochemical and histological study of the effect of antimicrobial photodynamic therapy on oral mucositis induced by 5-fluorouracil in hamsters, *Photodiagn. Photodyn. Ther.* 12 (2015) 298–309.
- [54] W. Lopes-Junior, V.G. Garcia, T. Okamoto, L.H. Theodoro, C.P. Eduardo, Repairing process in infected wounds dental extraction, treated with photosensitizer drug, associated or no the low intensity laser: histological study in mice, *J. Oral Laser Appl.* 1 (2001) 49.
- [55] J.M. De Almeida, L.H. Theodoro, A.F. Bosco, M.J. Nagata, M. Oshiiwa, V.G. Garcia, Influence of photodynamic therapy on the development of ligature-induced periodontitis in rats, *J. Periodontol.* 78 (2007) 566–575.
- [56] J.M. De Almeida, L.H. Theodoro, A.F. Bosco, M.J. Nagata, S. Bonfante, V.G. Garcia, Treatment of experimental periodontal disease by photodynamic therapy in rats with diabetes, *J. Periodontol.* 79 (11) (2008) 2156–2165.
- [57] L.A. Fernandes, J.M. De Almeida, L.H. Theodoro, A.F. Bosco, M.J. Nagata, T.M. Martins, T. Okamoto, V.G. Garcia, Treatment of experimental periodontal disease by photodynamic therapy in immunosuppressed rats, *J. Clin. Periodontol.* 36 (3) (2009) 219–228.
- [58] V.G. Garcia, E.C. Gualberto Júnior, L.A. Fernandes, A.F. Bosco, M.J. Hitomi Nagata, C.A. Casatti, E. Ervolino, L.H. Theodoro, Adjunctive antimicrobial photodynamic treatment of experimentally induced periodontitis in rats with ovariectomy, *J. Periodontol.* 84 (4) (2013) 556–565.
- [59] V.G. Garcia, L.A. Fernandes, V.C. Macarini, J.M. De Almeida, T.M. Martins, A.F. Bosco, M.J. Nagata, J.A. Cirelli, L.H. Theodoro, Treatment of experimental periodontal disease with antimicrobial photodynamic therapy in nicotine-modified rats, *J. Clin. Periodontol.* 38 (12) (2011) 1106–1114.
- [60] L.H. Theodoro, M. Longo, E. Ervolino, M. Ferro-Alves, N. Assem, M.J. Nagata, J.M. De Almeida, V.G. Garcia, aPDT for treatment of periodontitis in rats subjected to chemotherapy, *J. Dent. Res.* 94A (2015) 1728.
- [61] J.A. Dos Reis Jr., J.N. Dos Santos, B.S. Barreto, P.N. De Assis, P.F. Almeida, A.L. Pinheiro, Photodynamic antimicrobial chemotherapy (PACT) in osteomyelitis induced by *Staphylococcus aureus*: microbiological and histological study, *J. Photochem. Photobiol. B* 149 (2015) 235–242.
- [62] J.A. Dos Reis Jr., F.B. De Carvalho, R.F. Trindade, P.N. De Assis, P.F. De Almeida, A.L. Pinheiro, A new preclinical approach for treating chronic osteomyelitis induced by *Staphylococcus aureus*: in vitro and in vivo study on photodynamic antimicrobial therapy (PAmT), *Lasers Med. Sci.* 29 (2014) 789–795.
- [63] F. Hallmer, T. Bjørnland, G. Andersson, J.P. Becktor, A.K. Kristoffersen, M. Enersen, Bacterial diversity in medication-related osteonecrosis of the jaw, *Oral Surg. Oral Med. Oral Pathol. Oral Radiol.* 123 (4) (2017) 436–444.
- [64] H. Mawardi, G. Giro, M. Kajiya, K. Ohta, S. Almazrooa, E. Alshwaimi, S.B. Woo, I. Nishimura, T. Kawai, A role of oral bacteria in bisphosphonate-induced osteonecrosis of the jaw, *J. Dent. Res.* 90 (11) (2011) 1339–1345.
- [65] S. Panya, R. Fliefel, F. Probst, M. Tröltzsch, M. Ehrenfeld, S. Schubert, S. Otto, Role of microbiological culture and polymerase chain reaction (PCR) of *Actinomyces* in medication-related osteonecrosis of the jaw (MRONJ), *J. Craniomaxillofac. Surg.* 45 (2017) 357–363.
- [66] G. Russmueller, R. Seemann, K. Weiss, V. Stadler, M. Speiss, C. Perisanidis, T. Fuereder, B. Willinger, I. Sulzbacher, C. Steininger, The association of medication-related osteonecrosis of the jaw with *Actinomyces* spp. infection, *Sci. Rep.* 6 (2016) 31604.
- [67] C.L. Li, C.J. Seneviratne, L. Huo, W.W. Lu, L.W. Zheng, Impact of *Actinomyces naeslundii* on bisphosphonate-related osteonecrosis of the jaws in ovariectomized rats with periodontitis, *J. Craniomaxillofac. Surg.* 43 (2015) 1662–1669.
- [68] S. Hafner, M. Ehrenfeld, E. Storz, A. Wieser, Photodynamic inactivation of *Actinomyces naeslundii* in comparison with chlorhexidine and polyhexanide—a new approach for antiseptic treatment of medication-related osteonecrosis of the jaw? *J. Oral Maxillofac. Surg.* 74 (2016) 516–522.